



**HAL**  
open science

## Cobalt Doping Effect on Ni-Zn-Cu Ferrites Produced by Reactive Sintering

Adrien Mercier, Gérard Chaplier, Alexandre Pasko, Vincent Loyau, Frédéric  
Mazaleyrat

► **To cite this version:**

Adrien Mercier, Gérard Chaplier, Alexandre Pasko, Vincent Loyau, Frédéric Mazaleyrat. Cobalt Doping Effect on Ni-Zn-Cu Ferrites Produced by Reactive Sintering. *Physics Procedia*, 2015, 75, pp.1306 - 1313. 10.1016/j.phpro.2015.12.146 . hal-01448858

**HAL Id: hal-01448858**

**<https://hal.science/hal-01448858>**

Submitted on 29 Jan 2017

**HAL** is a multi-disciplinary open access archive for the deposit and dissemination of scientific research documents, whether they are published or not. The documents may come from teaching and research institutions in France or abroad, or from public or private research centers.

L'archive ouverte pluridisciplinaire **HAL**, est destinée au dépôt et à la diffusion de documents scientifiques de niveau recherche, publiés ou non, émanant des établissements d'enseignement et de recherche français ou étrangers, des laboratoires publics ou privés.



# Cobalt doping effect on Ni-Zn-Cu ferrites produced by reactive sintering

Adrien Mercier<sup>1</sup>, Gérard Chaplier<sup>1</sup>, Alexandre Pasko<sup>1</sup>, Vincent Loyau<sup>1</sup> and Frédéric Mazaleyrat<sup>1</sup>

<sup>1</sup>SATIE, ENS Cachan, CNRS, Université Paris-Saclay, 61 av Président Wilson, F-94230, France  
adrien.mercier@satie.ens-cachan.fr

## Abstract

This work deals with the Ni-Zn-Cu ferrites for energy conversion. Studies have already shown the beneficial effects of substituting some of divalent ions by  $\text{Co}^{2+}$ . Particularly, it appears that with a small amount of cobalt, it is possible to increase the permeability and to reduce magnetic losses. In this paper, our goal is to report if these properties are still valid with another manufacturing process: the spark plasma sintering. This process can be used for reactive sintering where it is possible to synthesize and to sinter the material in a single step in order to greatly reduce production time.

*Keywords:* Ferrites, SPS, Reactive Sintering

## 1 Introduction

It is well established that the use of spinel ferrite has led to important contributions in energy conversion and electromagnetic compatibility filter. These materials are particularly useful for everyday domestic and industrial magnetic circuits. Indeed, their good behaviors at high frequencies have contributed to the design of modern electronic systems. Among all the families of spinel ferrite, the Ni-Zn type is of particular interest in the 100 kHz-10 MHz bandwidth. From the mid 90's, the special case of Ni-Zn-Cu ferrite have been widely used due to their low sintering temperature. On the other hand, cobalt substitution was investigated among this spinel ferrite family in order to improve magnetic properties, such as permeability or magnetic losses [1].

However, the aforementioned (and even electrical and mechanical) properties critically depend on the synthesis route and the sintering process. For example, it is well known that sintering at high temperatures increases the grain size leading to an increase of the permeability related to grain growth and porosity reduction. But getting high density at low sintering temperature requires fine grained powders, ideally below 100 nm. Many researches focus on alternative physical and chemical routes to produce ferrite nanopowders. Non-exhaustively, one can cite the laser target evaporation [2, 3], different soft chemical routes like co-precipitation [4] or polyol [5]. However, these techniques,

despite their efficiency, are drastically different from current industrial techniques which are based on the solid route only. Another possibility to sinter at low temperature is to use the spark plasma sintering (SPS) process. SPS allows to sinter in an efficient way (heating rates over 100 K/min and overall duration of several tens of minutes) and to decrease the sintering temperature by about 100 K due to the uniaxial pressure [6] and diffusion enhancement which is not yet clearly understood.

In this paper, we propose a first analysis in terms of complex initial permeability, Curie temperature, coercivity and saturation polarization of a Co-substituted Ni-Zn-Cu ferrite made by SPS process. We highlight the cobalt doping effect in comparison with classical methods and some current difficulties for which we proposed some future solutions.

## 2 Sample preparation

For this study, we have chosen to analyze the ferrites which have the following chemical composition:  $\text{Co}_x(\text{Ni}_{0.24}\text{Cu}_{0.2}\text{Zn}_{0.56})_{1-x}\text{Fe}_2\text{O}_4$  where the Co-substitution  $x$  varies from 0 to 0.07. We used simple oxide powders from Sigma-Aldrich. The mixture of these oxides is made by ball milling with a planetary mill. We used the Pulverisette 7 model from Fritsch. Typically, the grinding takes 30 minutes with a rotational speed of 400 rpm. The grinding bowl contains 18 balls each with a diameter of 7 mm and a mass of 1.4 grams for 5.5 grams of powder. Subsequently, the samples are prepared using spark plasma sintering: the mixture of simple oxides is placed in a graphite die between two pistons under 50 MPa of uniaxial pressure. The heat treatment with respect to the time is shown on Figure 1.

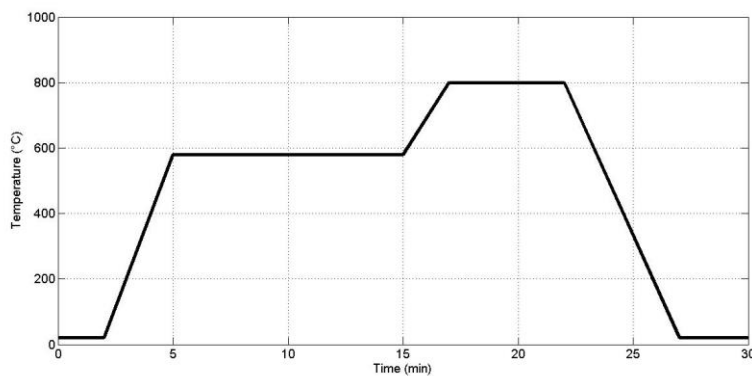


**Figure 1: Heat treatment with respect to the time.**

At the first step, the temperature is around 580 °C. At this stage, a chemical transformation occurs: the simple oxides react and the spinel phase is created. The second step, at around 800 °C, corresponds to the sintering, *i.e.* that the powder consolidates to form a solid. The produced ferrite samples are cylindrical, with a diameter of 8 mm, a thickness of about 3 mm and a weight of about 0.8 grams.

## 3 Experimental results

### 3.1 Structural analysis

With the SPS process, it is possible to control the grain size rather independently of the density. Indeed, the grain size is mainly dependent on temperature, whereas the density is essentially time dependent. In order to obtain a large bandwidth for a high frequency power electronic application, the

process was optimized to create submicrometric grains and high density. The heating profile was chosen from previous experiments [6]. In Figure 2, scanning electron microscope (SEM) images confirm that the desired microstructure is obtained: all grains are below 1  $\mu\text{m}$  with a quite large grain size distribution with an average of about several hundred nm.

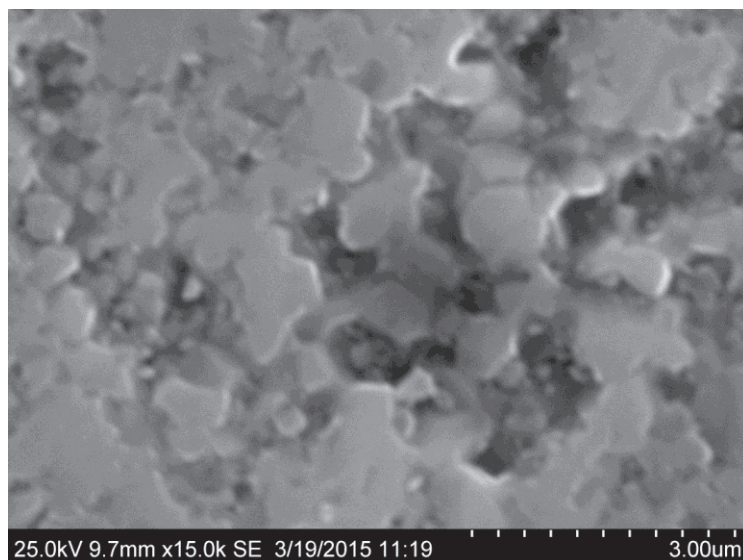


Figure 2: SEM picture of SPS sample with  $x = 0.06$ . Other samples show similar features.

X-ray patterns, obtained using a PANalytical X'Pert Pro diffractometer with Co  $K\alpha$  radiation. As expected for such low substitutions, all diffractograms are very similar. They show that the spinel phase occupies 95% of volume, the rest corresponds to unreacted simple oxides. The lattice parameter is 841 pm and the grain size, calculated from Debye-Scherrer formula is about 300 nm. The latter value is in rather good agreement with the SEM observation.

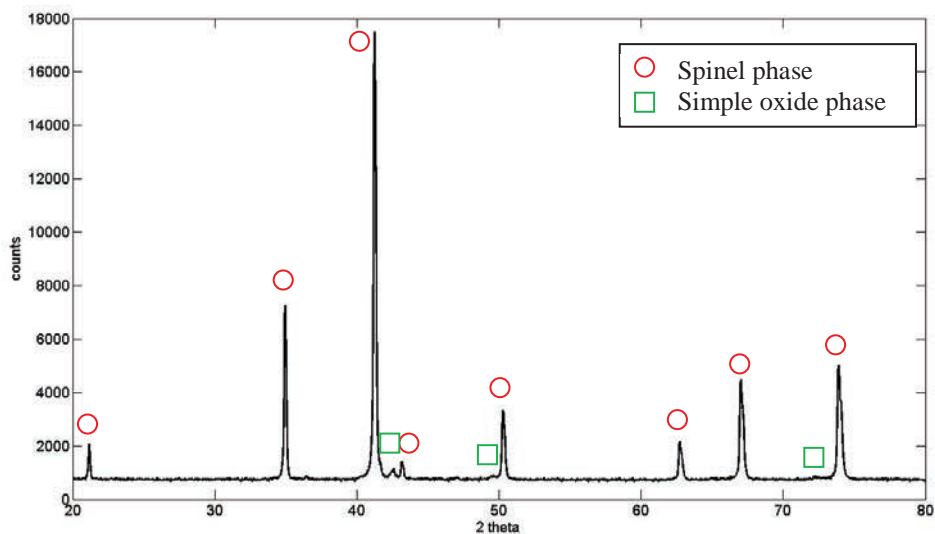
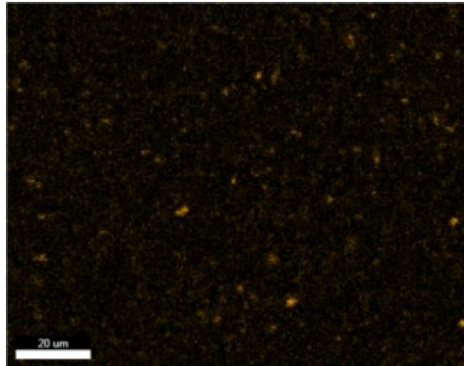


Figure 3: Example of X-ray diffractogram obtained for sample with  $x = 0.06$ .

In order to verify the presence of a secondary phase, the energy-dispersive X-ray spectroscopy (EDS) was used. An elemental map is shown in Figure 4 where nickel spots are clearly seen. As oxygen is also present in these regions with other elements absent, they should correspond to unreacted NiO. This observation is in agreement with X-ray diffraction patterns.



**Figure 4: EDS elemental map. Nickel spots appear in yellow.**

The size dispersion of the nickel-rich regions shows the inhomogeneity of samples. Some of these regions are about 2  $\mu\text{m}$ , which is larger than the average grain size. In principle, these NiO inclusions should not significantly influence the intrinsic magnetic properties of the spinel, but they can have positive effect on the macroscopic magnetic properties, affecting the permeability, as they produce internal demagnetization and the coercivity as they can pin domain walls.

### 3.2 Impedance spectrometry

For the other experiments, the samples are drilled in the center to obtain toroids. We measure the initial complex permeability using a HP 4195A spectrum analyzer with a coaxial cell. In Figure 5, one superimposes the real and imaginary parts of the permeability with respect to frequency.

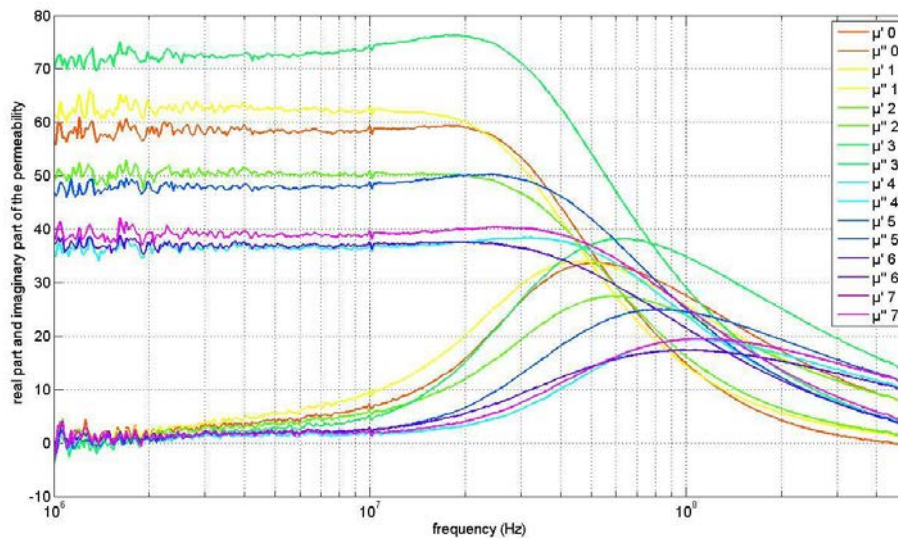


**Figure 5: Initial permeability spectrum.**

Each couple of curves with same color represents a number which corresponds to the degree of cobalt substitution in the ferrite. Concerning the real part of the permeability, one can see an important influence of the cobalt substitution. Indeed, at low frequency (around 1 MHz), the values vary from 40 to 75. Unfortunately, no tendency is clearly exhibited. However, the maximum of the permeability is achieved for 0.03 moles of cobalt:  $\text{Co}_{0.03}(\text{Ni}_{0.24}\text{Cu}_{0.2}\text{Zn}_{0.56})_{0.97}\text{Fe}_2\text{O}_4$ . This result is in agreement with the recent results [7] where only a classical sintering was performed.

### 3.3 Magnetic measurements

In order to determine the dependence of magnetic properties on temperature, the flux-metric method is used. Toroids have been wound primary and secondary together with 10 turns. For each sample and each temperature, a maximum magnetic field of 3000 A/m at frequency of 200 Hz is applied on the primary winding. The voltage is measured on the secondary winding and used to obtain the magnetic polarization.

To determine the Curie temperature, the cube of the polarization was plotted as a function of temperature (see Figure 6) for different amounts of cobalt. Empirically, one uses the most linear part segment in this zone. For the samples  $\text{Co}_0(\text{Ni}_{0.24}\text{Cu}_{0.2}\text{Zn}_{0.56})_1\text{Fe}_2\text{O}_4$ ,  $\text{Co}_{0.03}(\text{Ni}_{0.24}\text{Cu}_{0.2}\text{Zn}_{0.56})_{0.97}\text{Fe}_2\text{O}_4$  and  $\text{Co}_{0.07}(\text{Ni}_{0.24}\text{Cu}_{0.2}\text{Zn}_{0.56})_{0.93}\text{Fe}_2\text{O}_4$  a Curie temperature of around 140 °C, 95 °C and 105 °C, respectively, was determined. This technique is quite tricky as it depends on a good deal from men's appreciation. This result is not in line with [8] as a very slight increase in  $T_C$  was observed in this reference. This may be partly explained by the lack of nickel in the lattice due to unreacted NiO.

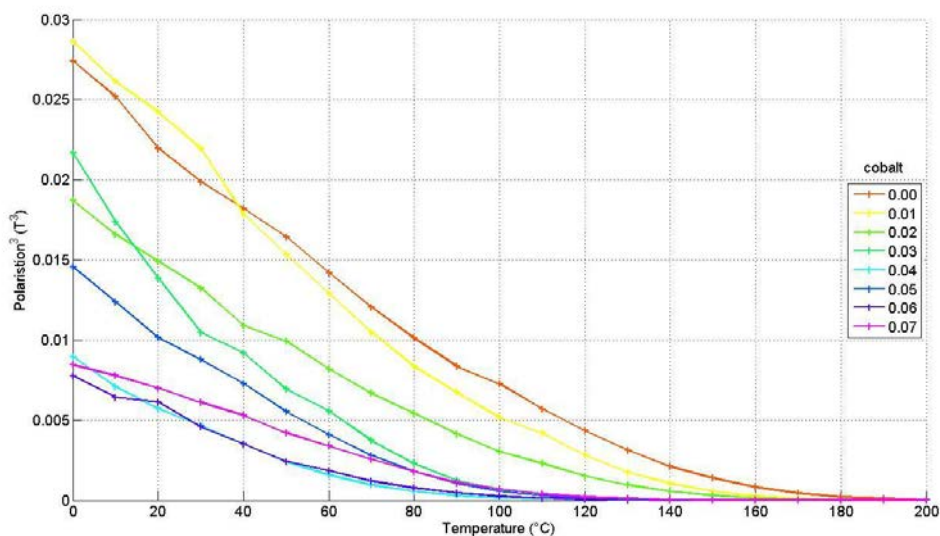


**Figure 6: Determination of the Curie temperature.**

To determine the influence of cobalt on the coercivity, the flux-metric measurement is still used. A magnetic field of 3000 A/m with a frequency of 200 Hz is applied on the primary winding. For each temperature, the coercivity can be determined from the hysteresis loop. The results are shown in Figure 7.

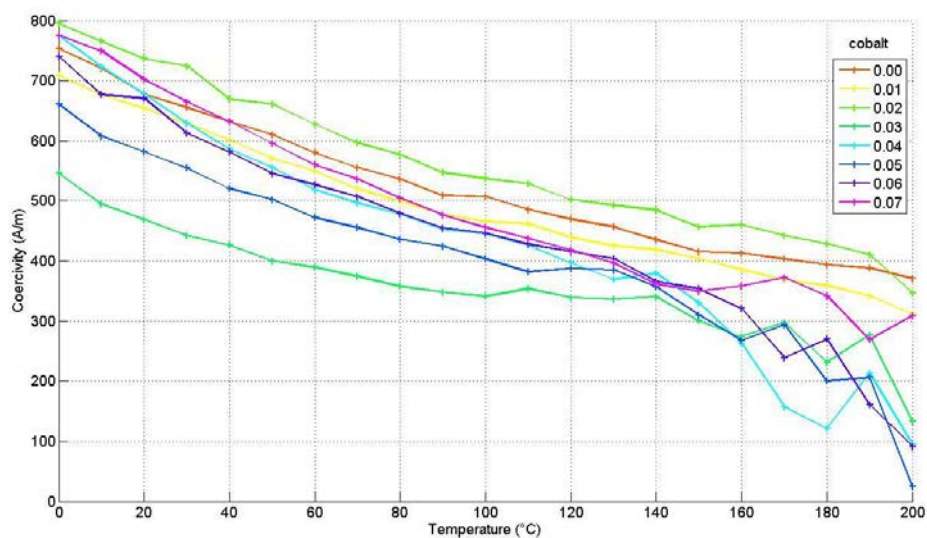


Figure 7: Coercivity as a function of temperature.

These measurements have to be compared with the measurements obtained in Figure 5. One can notice the interesting fact that the higher the permeability the lower the coercivity. Above 150 °C it is difficult to properly measure the coercivity because the hysteresis loop is too small.

In order to measure the saturation polarization, we used a LakeShore VSM. The results are shown in Figure 8.

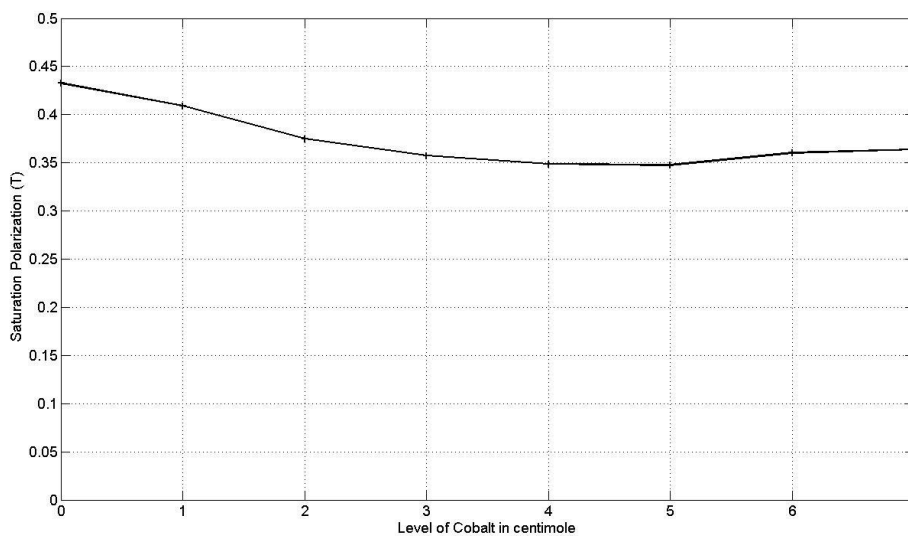


Figure 8: Saturation polarization for each sample at room temperature.

Contrary to other measurements, one can see that the cobalt substitution degree do not have a drastic influence on the saturation polarization.

The measured values of static initial permeability, relaxation frequency and saturation polarization at room temperature for  $\text{Co}_x(\text{Ni}_{0.24}\text{Cu}_{0.2}\text{Zn}_{0.56})_{1-x}\text{Fe}_2\text{O}_4$  samples ( $x = 0$  to 0.07) synthesized by SPS, are listed in Table 1 and compared with those prepared using conventional solid process [8].

The ferrites prepared by SPS method revealed similar magnetic properties to those obtained by conventional process, particularly with respect to the figure of merit  $\mu_i \times f_r$ . In addition, it is clearly seen that the SPS method requires lower temperature and a shorter time of sintering to obtain the Ni-Zn-Cu ferrite with a good purity as seen from XRD analysis.

**Table 1: Comparison between the conventional sintering and SPS.**

Sintering process	$\mu_i$ static	$f_r$ (MHz)	$\mu_i \times f_r$ (GHz)	$J_s$ at 20 °C (T)	Sintering temp. (°C)	Sintering time (min)
Conventional	180 - 830	5.6 - 31.7	~5.5	0.40 - 0.43	935	120
SPS	35 - 75	50 - 100	~4.1	0.35 - 0.44	800	5

## 4 Conclusion

Due to good properties of the Ni-Zn-Cu ferrites in terms of permeability when cobalt substitution is used, in this paper we have studied an alternative way of sintering based on the spark plasma sintering. We have provided an analysis in terms of complex initial permeability, Curie temperature, coercivity and saturation polarization. Our results show that a possible amelioration due to the cobalt is not yet clearly identified. However, the magnetic characteristics obtained by SPS are of the same order of magnitude as those obtained by conventional sintering, that is an interesting result for this relatively new way of sintering. A possible way to achieve homogeneous samples is currently under investigation and will be based on an optimization of the grinding parameters. Indeed, we will increase the rotation speed of the planetary mill in order to obtain finer powder to facilitate the sintering. Moreover, it could be interesting to measure the magnetic losses in order to know if this process allows an industrial production for power electronic.

## References

- [1] T. Y. Byun, S. C. Byeon, K. S. Hong and C. K. Kim. (1999). Factors affecting initial permeability of Co-substituted Ni-Zn-Cu ferrites. *IEEE Transactions on Magnetics*, 35, 3445-3447.
- [2] V. V. Osipov, V. V. Platonov, M. A. Uimin and A. V. Podkin (2012). Laser synthesis of magnetic iron oxide nanopowders. *Technical Physics*, 57(4), 543-549.
- [3] A. P. Safronov, I. V. Beketov, S. V. Komogortsev, G. V. Kurlyandskaya, A. I. Medvedev, D. V. Leiman, A. Larrañaga and S. M. Bhagat, (2013). Spherical magnetic nanoparticles fabricated by laser target evaporation. *AIP Advances*, 3(5), 052135.
- [4] P. K. Chakrabarti, B. K. Nath, S. Brahma, S. Das, K. Goswami, U. Kumar, P. K. Mukhopadhyay, D. Das, M. Ammar and F. Mazaleyrat. Magnetic and hyperfine properties of nanocrystalline

Ni<sub>0.2</sub>Zn<sub>0.6</sub>Cu<sub>0.2</sub>Fe<sub>2</sub>O<sub>4</sub> prepared by a chemical route. *Journal of Physics: Condensed Matter*, 18 (2006) 5253.

[5] R. Valenzuela, Z. Beji, F. Herbst, and S. Ammar. (2011). Ferromagnetic resonance behavior of spark plasma sintered Ni–Zn ferrite nanoparticles produced by a chemical route. *Journal of Applied Physics* 109.7 : 07A329.

[6] K. Zehani, F. Mazaleyrat, V. Loyau and E. Labouré. (2011). Effect of temperature and time on properties of Spark Plasma Sintered NiCuZn: Co ferrite. *Journal of Applied Physics*, 109(7), 07A504, *J. App. Phys.* **109**, 07A504 (2011)

[7] A. Lucas, R. Lebourgeois, F. Mazaleyrat and E. Labouré. (2010). Temperature dependence of spin resonance in cobalt substituted NiZnCu ferrites. *Applied Physics Letters*, 97, 182502.

[8] A. Lucas. PhD Theses. <https://tel.archives-ouvertes.fr/tel-00505792/document> . page 83